Supplementary Information

CryoEM analysis reveals human SID1 transmembrane family member1 dynamics underlying lipid hydrolytic activity

Authors

Yoshinori Hirano[1], Umeharu Ohto[1], Ryota Sato[2], Kensuke Miyake[2], Toshiyuki Shimizu[1]

Affiliations

[1]Graduate School of Pharmaceutical Sciences, The University of Tokyo, 7-3-1 Hongo, Bunkyo-ku, Tokyo, 113-0033, Japan.

[2]Division of Innate Immunity, Department of Microbiology and Immunology, The Institute of Medical Science, The University of Tokyo, 4-6-1 Shirokanedai, Minato-ku, Tokyo, 108-8639, Japan.

*Corresponding author:

Toshiyuki Shimizu (T.S.) Email: shimizu@mol.f.u-tokyo.ac.jp

This file includes

Supplementary Table 1

Supplementary Figure legends 1-12

	Human SIDT1 (closed-form) PDB 8KCW	Human SIDT1 in the presence of 25 bp dsRNA (open-form) PDB 8KCX
Data collection and processing		
Magnification	105,000	105,000
Voltage (kV)	300	300
Electron exposure (e^{-}/Å^2)	65.8	61.5
Defocus range (μm)	–0.8 to -1.6	-0.8 to -1.6
Pixel size (Å)	0.83	0.83
No. of micrographs	3297	5,002
Symmetry imposed	C_2	C_2
Initial particle images (no.)	2,180,197	2,383,232
Final particle images (no.)	59,745	62,617
Map resolution (Å)	2.77	2.96
FSC threshold	0.143	0.143
Map resolution range (Å)	2.77–10.0	2.96-10.0
Refinement		
Initial model used	*de novo*	
FSC threshold	0.5	0.5
Correlation coefficient (CCmask)	0.82	0.83
Model resolution range (Å)	2.77–10.0	2.96-10.0
Map sharpening *B* factor (Å^2)	74.7	74.5
Model composition		
Non-hydrogen atoms	10484	9486
Protein residues	1252	1142
Glycan residues (NAG, BMA)	20	20
Cholesterols	2	0
Ions (Zn)	2	2
B factors (Å^2)		
Protein	93.0	109.0
Glycan residues (NAG, BMA)	34.3	156.6
Cholesterol	52.4	
Ions (Zn)	129.6	138.8
R.m.s. deviations		
Bond lengths (Å)	0.005	0.004
Bond angles (°)	0.77	0.717
Validation		
MolProbity score	1.47	1.23
Clashscore	5.92	4.56
Poor rotamers (%)	0.18	0.00
Ramachandran plot		
Favored (%)	97.24	98.20
Allowed (%)	2.76	1.80
Disallowed (%)	0.00	0.00

Supplementary Table 1 Cryo-EM data collection, refinement, and validation statistics


β1
β2
β3
β4
β5
β6
β7
β8
β9
β10
β11
β12
β13
β14
β15
β16
β17
β18
TM1
TM2
TM3
TM4
hSIDT1 MRGCLRLALLCALPWLLLAASPGHPAKSPRQPPAPRRDPFDAARGADFDHVYSGVVNLSTENIYSFNYTS 70
mSIDT1 MLDCLRLALLCALPWLLRAAVPGHQEEPLAKSAELRRDPRDPARGADFDRVYSGVVSLSTENIYSFNHTS
hSIDT2 -------MFALGLPFLVLLVASVESHLGVLGP------KNVSQKDAEFERTYVDEVNSELVNIYTFNHTV
mSIDT2 -------MIAWRLPLCVLLVASVESHLGALGP------KNVSQKDAEFERTYADDVNSELVNIYTFNHTV
cSID-1 ---MIRVYLI-ILMHLVIGLT—QNNSTTPSPIITSSNSSVLVFEISSKMKMIEKKLE—ANTVHVLRLE
hSIDT1 Q—PDQVTAVRVYVNSSS----ENLNYPVLVVVRQQ-KEVLSWQVPLLFQGLYQRSYNYQEVSRTLCPSE 133
mSIDT1 H—PGQVTAVRVHVNSSS----DNLDYPVLVVVRQQ-KEVLSWQVPLLFQGLYQRSYNYQEVSRTLCPSK
hSIDT2 T—RNRTEGVRVSVNVLN----KQKGAPLLFVVRQK-EAVVSFQVPLILRGMFQRKYLYQKVERTLCQPP
mSIDT2 T—RNRTEGVRVSVNVLN----KQKGAPLLFVVRQK-EAVVSFQVPLILRGLYQRKYLYQKVERTLCQPP
cSID-1 LDQSFILDLTKVAAEIVDSSKYSKEDGVILEVTVSNGRDSFLLKLPTVYP-----NLKLYTDGKLLNPLV
hSIDT1 ATNETG----------PLQQLIFVDVASMAPLGAQYKLLVTKLKHFQ------LRTNVAFHFTAS---PS 184
mSIDT1 ATNETG----------PLEQLIFVDVASMAPHGAHYKLLVTKIKHFQ------LPTNVAFYFTAS---PS
hSIDT2 TKNE------------SEIQFFYVDVSTLSPVNTTYQLRVSRMDDFV------LRTGEQFSFNTT---AA
mSIDT2 TKNE------------SEIQFFYVDVSTLSPVNTTYQLRVNRVDNFV------LRTGELFTFNTT---AA
cSID-1 EQDFGAHRKRHRIGDPHFHQNLIVTVQSRLNADIDYRLHVTHLDRAQYDFLKFKTGQTTKTLSNQKLTFV
hSIDT1 QPQYFLYKFP-KDVDSVIIKVVSEMAYPCSVVSVQNIMCPVYDLDHN--VEFNGVYQSMTKKAAITLQKK 251
mSIDT1 QPQYFLYKFP-EDVDSVIIKVVSEKAYPCSVVSVQNIMCPVYDLDHN--VEFNGVYQSMTKKAAITLQKK
hSIDT2 QPQYFKYEFP-EGVDSVIVKVTSNKAFPCSVISIQDVLCPVYDLDNN--VAFIGMYQTMTKKAAITVQRK
mSIDT2 QPQYFKYEFP-DGVDSVIVKVTSKKAFPCSVISIQDVLCPVYDLDNN--VAFIGMYQTMTKKAAITVQRK
cSID-1 KPIGFFLNCSEQNISQFHVTLYSED-DICANLITVPANESIYDRSVISDKTHNRRVLSFTKRADIFFTET
hSIDT1 DFP-GEQFFVVFVIKPEDYACGGSFFIQE---------KENQTWNLQRKKNLEVTIVPSIKESVYVKSSL 311
mSIDT1 DFP-DEQFFVVFVIKPEDYACGGSFSIQE---------NENQTWNLQRSKNLKVTIVPSIKESVYVKSSL
hSIDT2 DFP-SNSFYVVVVVKTEDQACGGSLPFYP-------FAEDEPVDQGHRQKTLSVLVSQAVTSEAYVSGML
mSIDT2 DFP-SNSFYVVVVVKTEDQACGGSLPFYP-------FVEDEPVDQGHRQKTLSVLVSQAVTSEAYVGGML
cSID-1 EISMFKSFRIFVFIAPDDSGCSTNTSRKS----------------FNEKKKISFEFKKLENQSYAVPTAL
hSIDT1 FSVFIFLSFYLGCLLVGFVHYLRFQRKSIDGSFG---SNDGSGNMVASHPIAASTPEGSNYGTIDESSSS 378
mSIDT1 FSIFVFLSFYLGCLLVVLVHHVRFQRKSIDGSFG---SSDGSGNMAVSHPITASTPEGSNYGAIDESSSS
hSIDT2 FCLGIFLSFYLLTVLLACWENWRQKKKTLLVAIDRACPESGHPRVLADSFPGSSPYEGYNYGSFENVSGS
mSIDT2 FCLGIFLSFYLLTVLLACWENWRQRKKTLLLAIDRACPESGHARVLADSFPGSAPYEGYNYGSFENGSGS
cSID-1 -MMIFLTTCLLFLPIVINIIKNSRKLAP-------------SQSNLISFSPVPSEQRDMDL-------SH
hSIDT1 PGRQMSSS----------------DGGPPGQSDTDSSVEESDFDTMPDIESDKNIIRTKMFLYLSDLSRKD 433
mSIDT1 PGRQMSSS----------------DGGQPCHSDTDSSVEESDFDTMPDIESDKNVIRTKMFLYLSDLSRKD
hSIDT2 TDGLVDSAGTGDLSYGYQGRSFEPVGTRPRVDSMSSVEEDDYDTLTDIDSDKNVIRTKQYLYVADLARKD
mSIDT2 TDGLVESAGSGDLSYSYQDRSFDAVGPRPRLDSMSSVEEDDYDTLTDIDSDKNVIRTKQYLCVADLARKD
cSID-1 DEQQNTSS-------------ELENNGEIPAAENQIVEEITAENQETS------------VEEGNREIQV
hSIDT1 RRIVSKKYKIYFWNIITIAVFYALPVIQLVITYQTVVNVTGN---QDICYYNFLCAHPLGVLSAFNNILS 500
mSIDT1 RRIVSKKYKIYFWNIITIAVFYALPVMQLVITYQYVVNVTGN---QDICYYNFLCAHPLGVLSAFNNILS
hSIDT2 KRVLRKKYQIYFWNIATIAVFYALPVVQLVITYQTVVNVTGN---QDICYYNFLCAHPLGNLSAFNNILS
mSIDT2 KRVLRKKYQIYFWNIATIAVFYALPVVQLVITYQTVVNVTGN---QDICYYNFLCAHPLGNLSAFNNILS
cSID-1 KIPLKQDSLSLHGQMLQYPVAIILPVLMHTAIEFHKWTTSTMANRDEMCFHNHACARPLGELRAWNNIIT
hSIDT1 NLGHVLLGFLFLLIVLRRDILHRRALEAKDIFAVEYGIPKHFGLFYAMGIALMMEGVLSACYHVCPNYSN 570
mSIDT1 NLGHVLLGFLFLLIVLRRDLLHRRALEAKDIFAMEYGIPKHFGLFYAMGIALMMEGVLSACYHVCPNYSN
hSIDT2 NLGYILLGLLFLLIILQREINHNRALLRNDLCALECGIPKHFGLFYAMGTALMMEGLLSACYHVCPNYTN
mSIDT2 NLGYILLGLLFLLIILQREINHNRALLRNDLYALECGIPKHFGLFYAMGTALMMEGLLSACYHVCPNYTN
cSID-1 NIGYTLYGAIFIVLSICRRGRHEYSHVF----GTYEC----TLLDVTIGVFMVLQSIASATYHICPSDVA

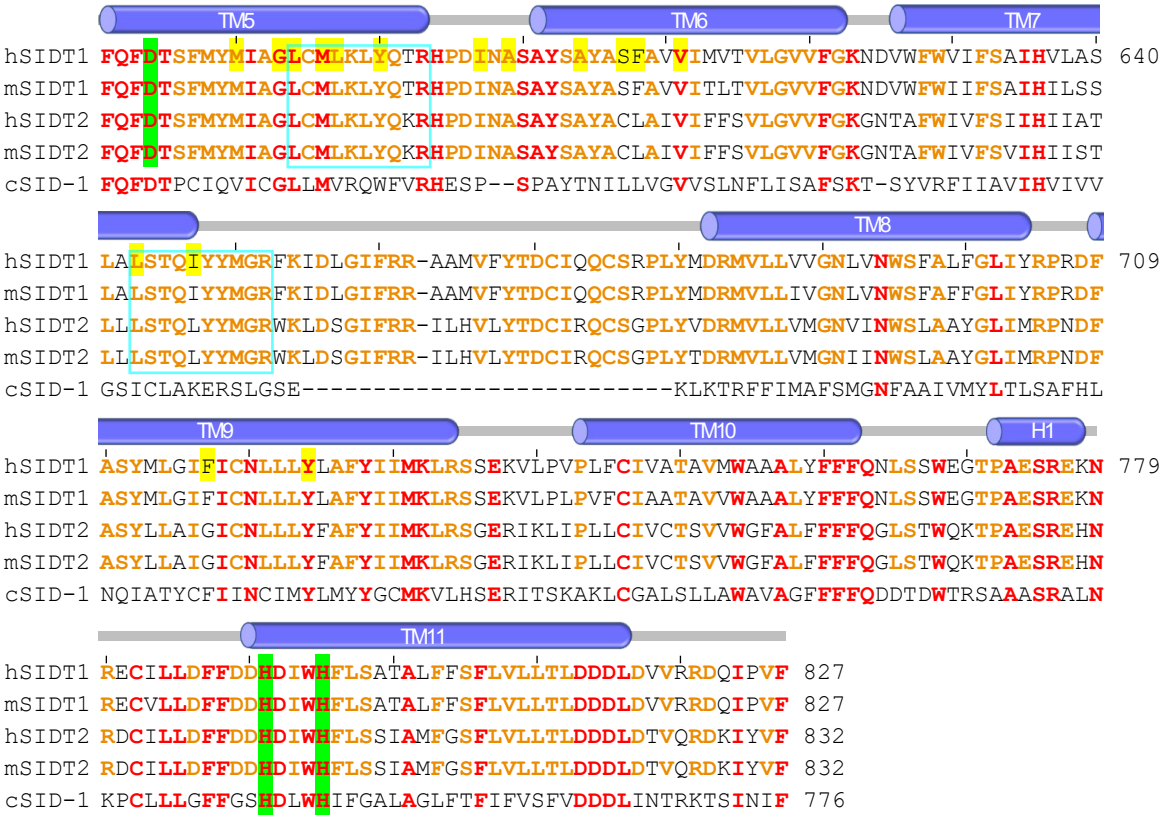

Supplementary Fig. 1 Sequence alignment of SID-1 family proteins.

Sequence alignment of human, mouse SIDT1/ SIDT2 as well as *C. elegans* SID-1were performed using Clustal Omega with a small manual modification. Secondary structures are indicated in arrow-head (β-sheet) or cylinder (helix) above the sequence of human SIDT1. Residues completely conserved in listed SID-1 family proteins are red while the residues conserved in listed mammalian SID-1 family proteins are shown in red and orange, respectively. The catalytic residues are highlighted in green. Residues involved in cholesterol binding is highlighted in yellow. The CRAC motifs in extracellular region (β10), TM5 and TM7 are boxed in cyan.

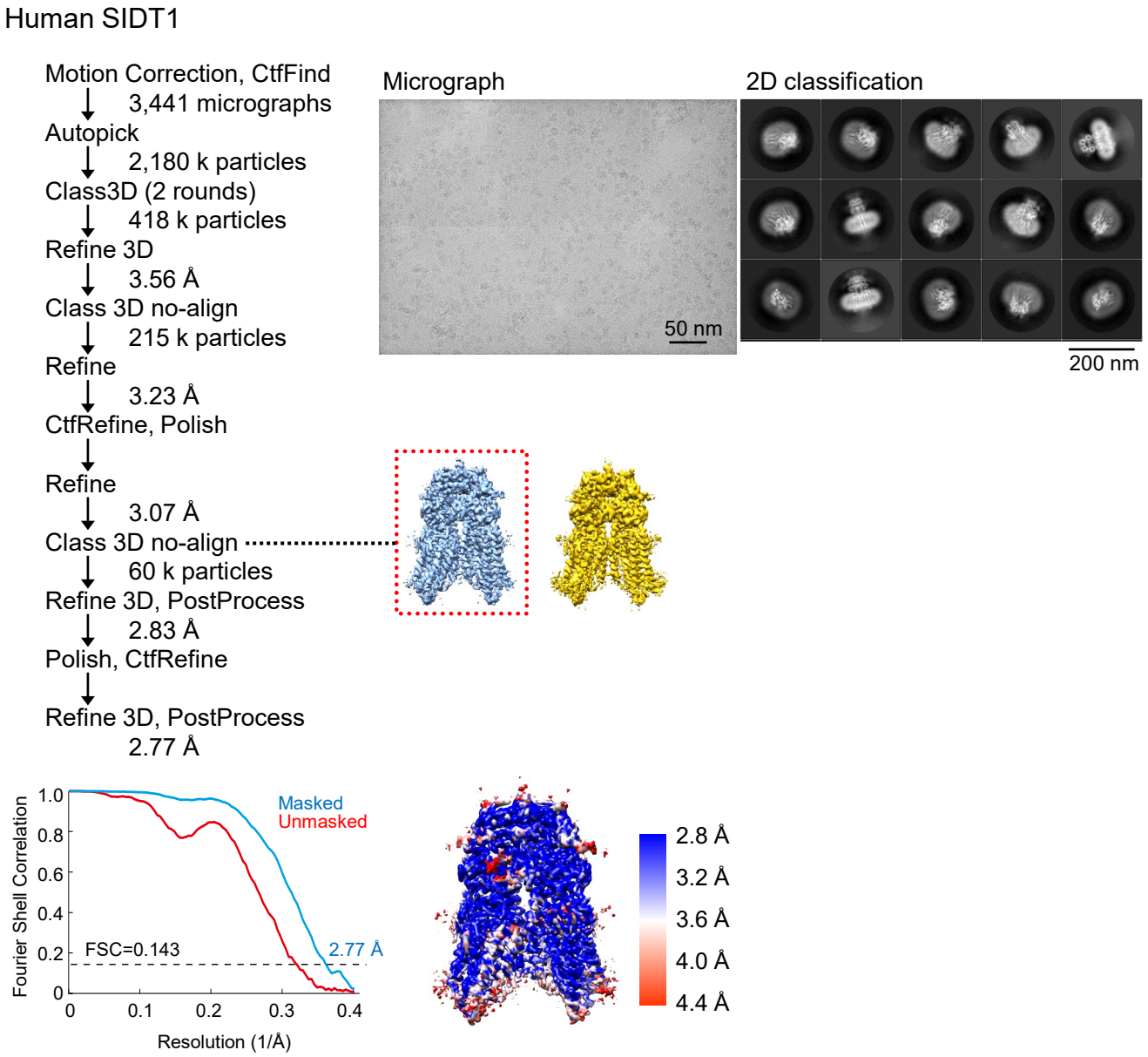

Supplementary Fig. 2 Cryo-EM analysis of human SIDT1.

Data processing workflow of cryo-EM analysis of human SIDT1. Representative motion-corrected micrograph out of 3,441 total micrographs, 3D class averages, gold-standard FSC curves of the final 3D reconstruction (resolution cut-off at FSC = 0.143), and the final 3D map (colored according to the local resolution) are shown. 2D class averages were calculated using refined particles that were used for the final reconstruction. 3D class selected for the following analyses are indicated with red dotted boxes.

Human SIDT1 in the presence of 25 bp dsRNA

Motion Correction, CtfFind
↓ 5,002 micrographs
Autopick
↓ 2,383k particles
Class3D (3 rounds)
↓ 682 k particles
Refine3D
↓ 3.72 Å
CtfRefine, Polish
↓
Refine3D, PostProcess
↓ 3.41 Å
Class 3D no-align
↓ 187 k particles
Refine
↓ 3.19 Å
CtfRefine, Polish
↓
Refine
↓ 3.04 Å
Class 3D no-align

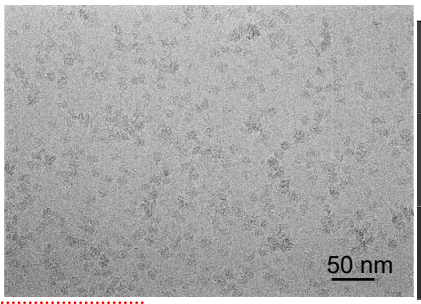

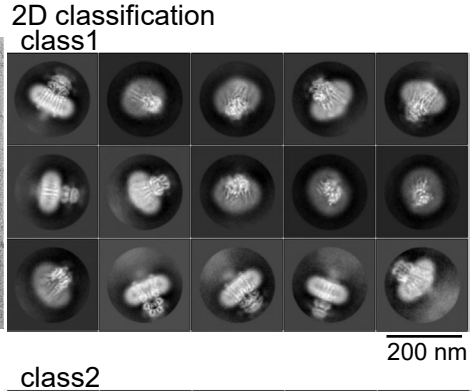

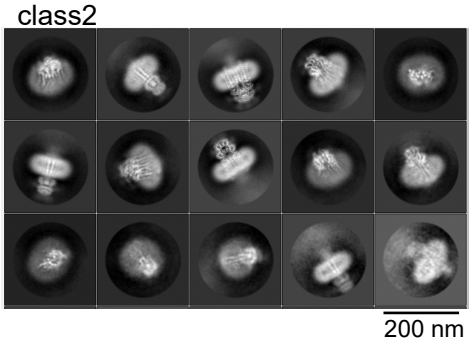

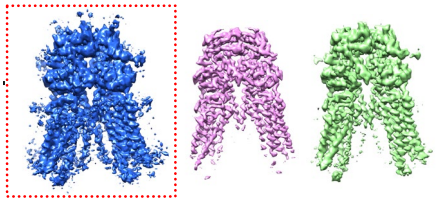

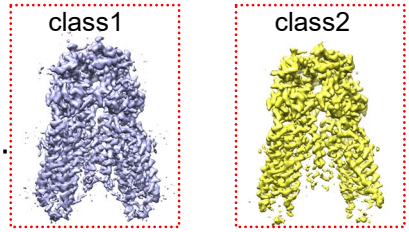

Class1 (closed-form)
↓ 50 k particles
Polish
↓
Refine 3D, PostProcess
2.86 Å

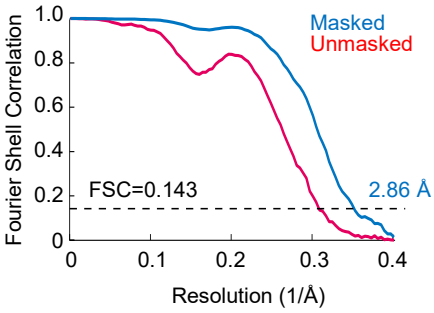

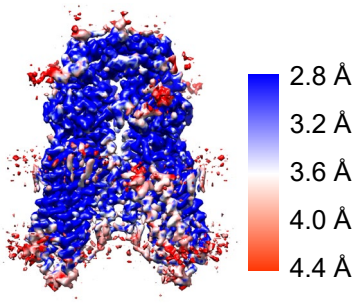

Class2 (open-form)
↓ 137 k particles
Class 3D
↓ 63 k particles
Refine 3D, PostProcess
↓
Polish
↓
Refine 3D, PostProcess
2.96 Å

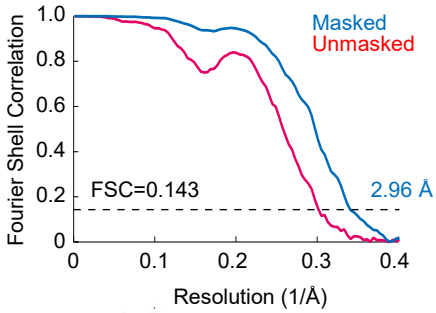

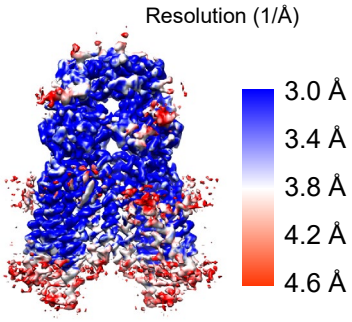

Supplementary Fig. 3 Cryo-EM analysis of human SIDT1 in the presence of 25 bp dsRNA.
Data processing workflow of cryo-EM analysis of human SIDT1 in the presence of 25 bp dsRNA. Representative motion-corrected micrograph out of 5,002 total micrographs, 3D class averages, gold-standard FSC curves of the final 3D reconstruction (resolution cut-off at FSC = 0.143), and the final 3D map (coloured according to the local resolution) are shown. 2D class averages were calculated using refined particles that were used for the final reconstruction. 3D class selected for the following analyses are indicated with red dotted boxes.

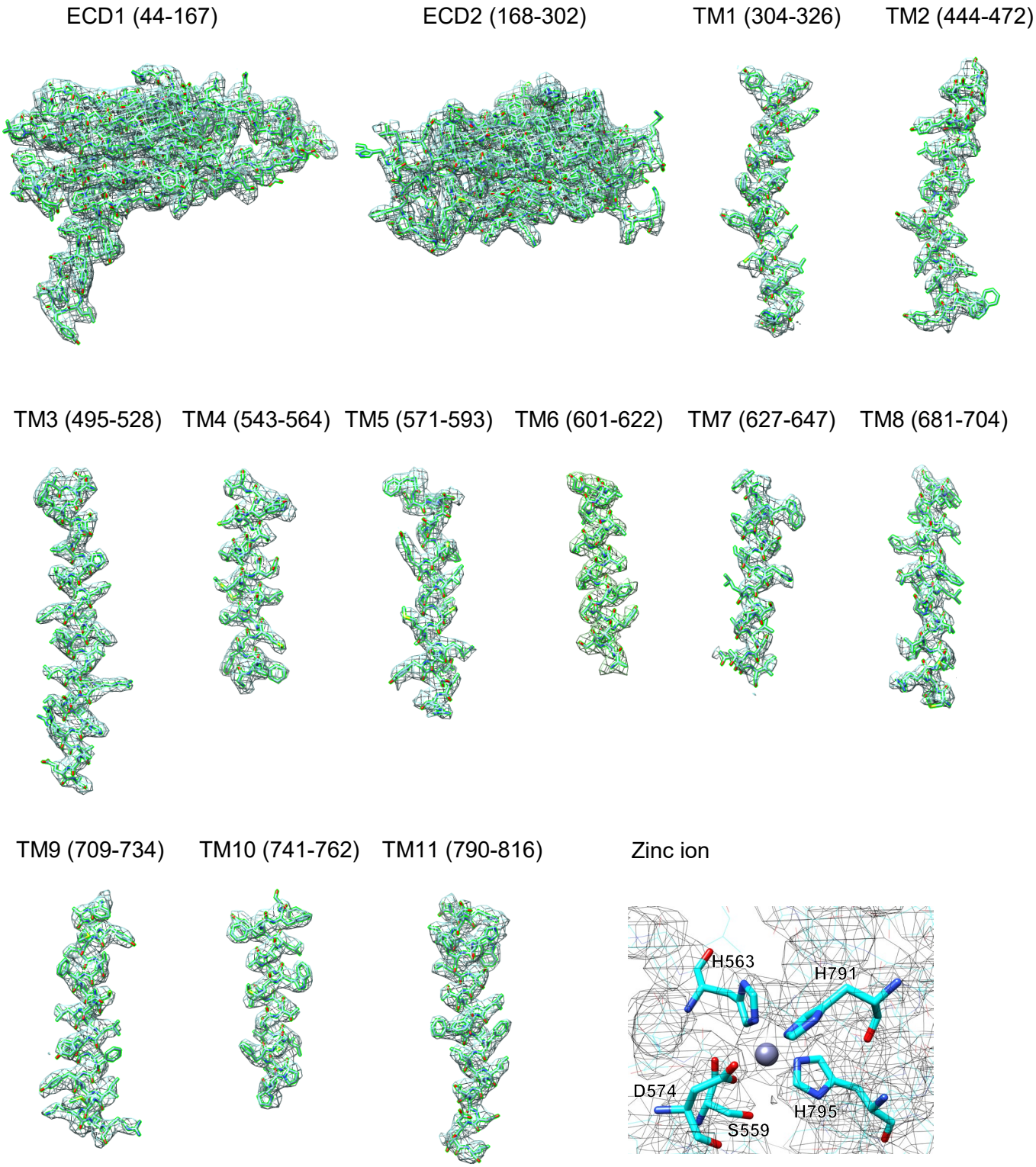

Supplementary Fig. 4 Representative density for the extracellular and transmembrane regions of the closed form of human SIDT1.

Representative cryo-EM density maps of the closed-form of human SIDT1 around ECD1, ECD2 and each TM helix of human SIDT1 and zinc ion are shown.

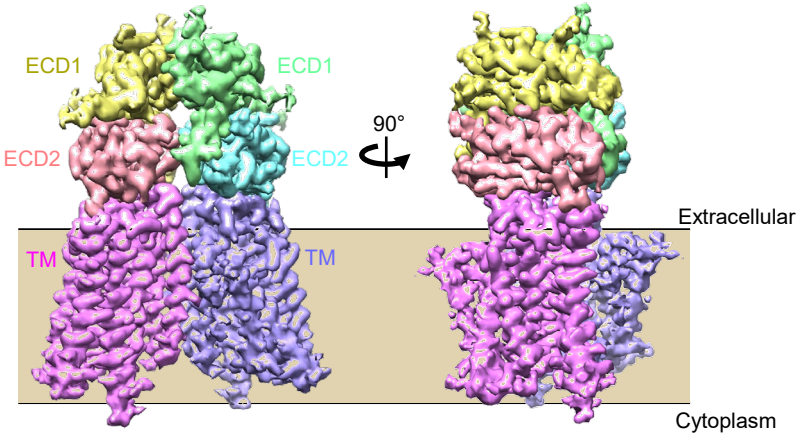

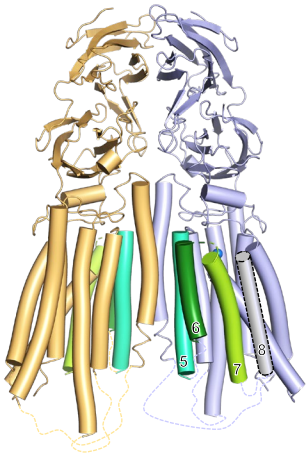

ECD1 (44-167)

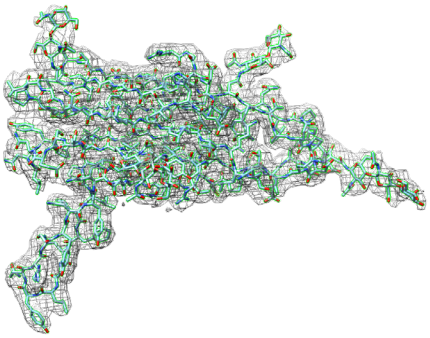

ECD2 (168-302)

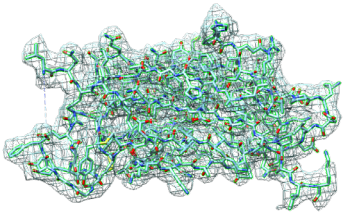

TM1 (303-334)

TM2 (449-472)

TM3 (495-527)

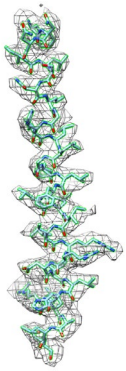

TM4 (542-564)

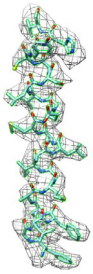

TM5 (568-591)

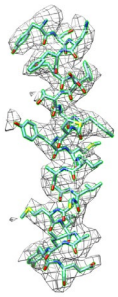

TM6 (606-620)

TM7 (627-650)

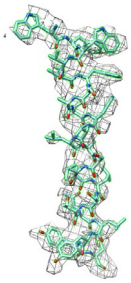

TM9 (710-734)

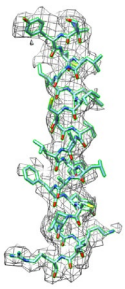

TM10 (741-762)

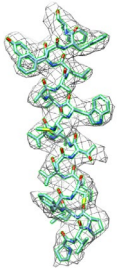

TM11 (790-810)

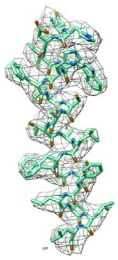

Zinc ion

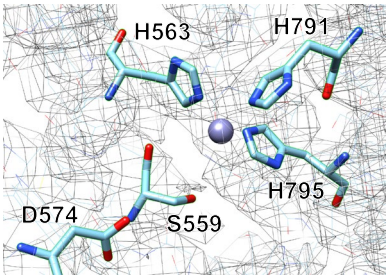

Supplementary Fig. 5 Representative density for the extracellular and transmembrane regions of the open-form of human SIDT1.

Representative cryo-EM density maps of the open-form of human SIDT1 around ECD1, ECD2 and each TM helix of human SIDT1 and zinc ion are shown.

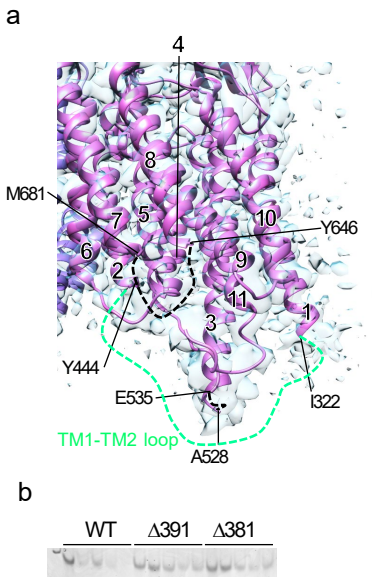

Supplementary Fig. 6 The structure of SIDT1 in the presence of dsRNA.
(a) The cytoplasmic region of hSIDT1 closed-form is shown. The TM1-TM2, TM3-TM4 and TM7-8 loops are discontinued, which indicated as dashed lines. The cytoplasmic TM1-TM2 loop is largely disordered in the cryo-EM map (green dashed line).
(b) EMSA assay using full length hSIDT1 or mutant with TM1-2 loop deletion (Δ391: 391-442, Δ381: 381-442). Unshifted band corresponding to unbound dsRNA was monitored to estimate dsRNA binding with SIDT1 since hSIDT1-dsRNA complex less migrated. Increasing concentration of hSIDT1 (1, 2, 3, 4, 5 μM) was incubated with 1 μM of dsRNA and subjected to electrophoresis.

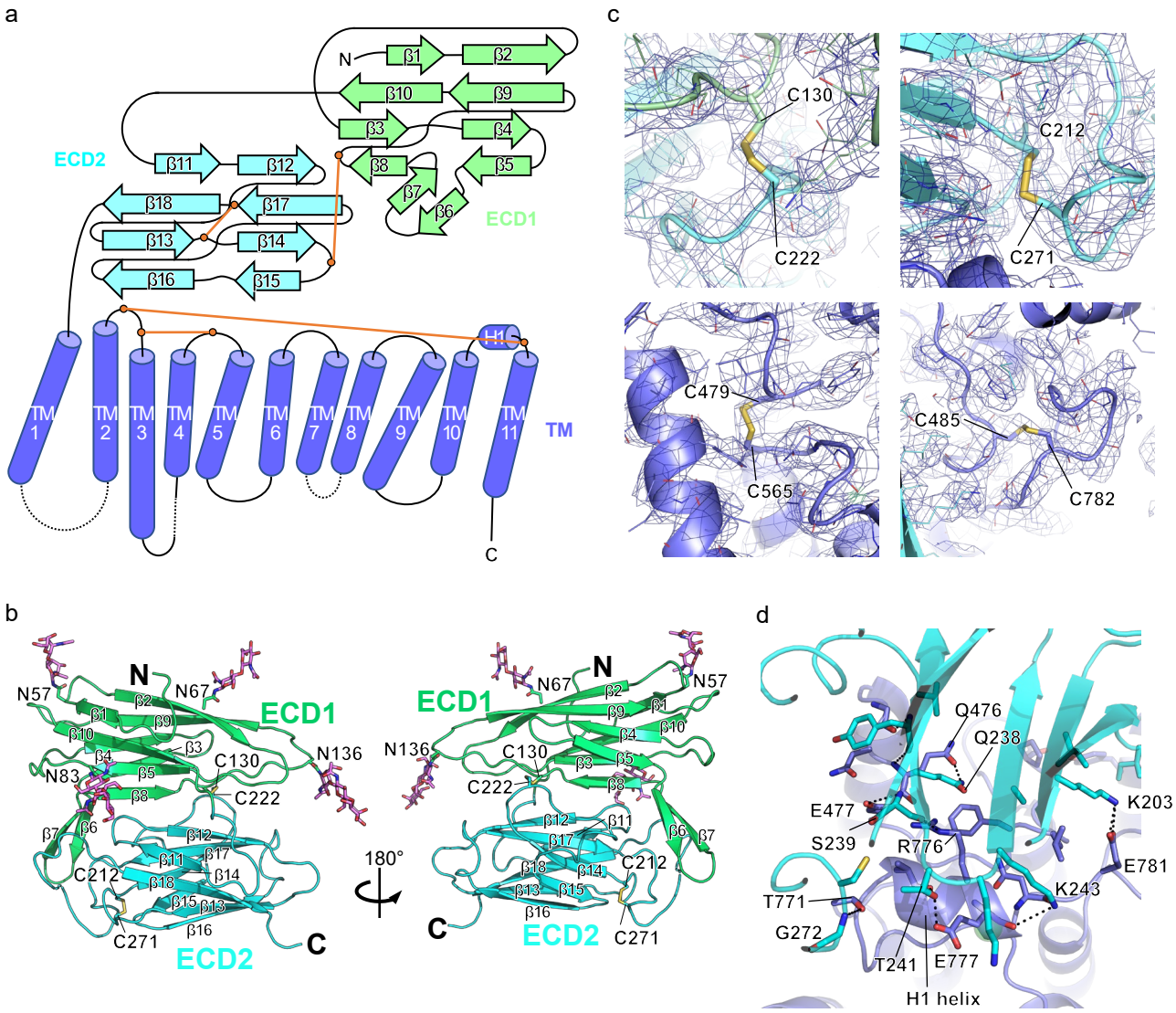

Supplementary Fig. 7 The assembly of extracellular region of SIDT1.

(a) Topology diagram of human SIDT1. Dotted lines indicate disordered regions in the cryo-EM map in the structure of human SIDT1 closed form. The β-strand and α-helix are shown in arrowhead and cylinder, respectively.

(b) Structure of the extracellular region of human SIDT1consists of 2 domains (ECD1 and ECD2) which adopt β-sandwich folds. The extracellular region has four N-glycosylation (Asn57, Asn67, Asn83 and Asn136) and two disulfide bonds (Cys130-Cys222 and Cys212-Cys271). ECD1 and ECD2 are tightly packed with each other.

(c) The cryo-EM densities around disulfide bonds are shown.

(d) The N-terminal extracellular domain is packed with TM segments through the interaction between ECD2 and TM2-TM3/TM10-TM10 loops. Residues that forms hydrogen bond or salt bridge (dotted line) are shown with label. Disulfide bonds are shown as orange lines.

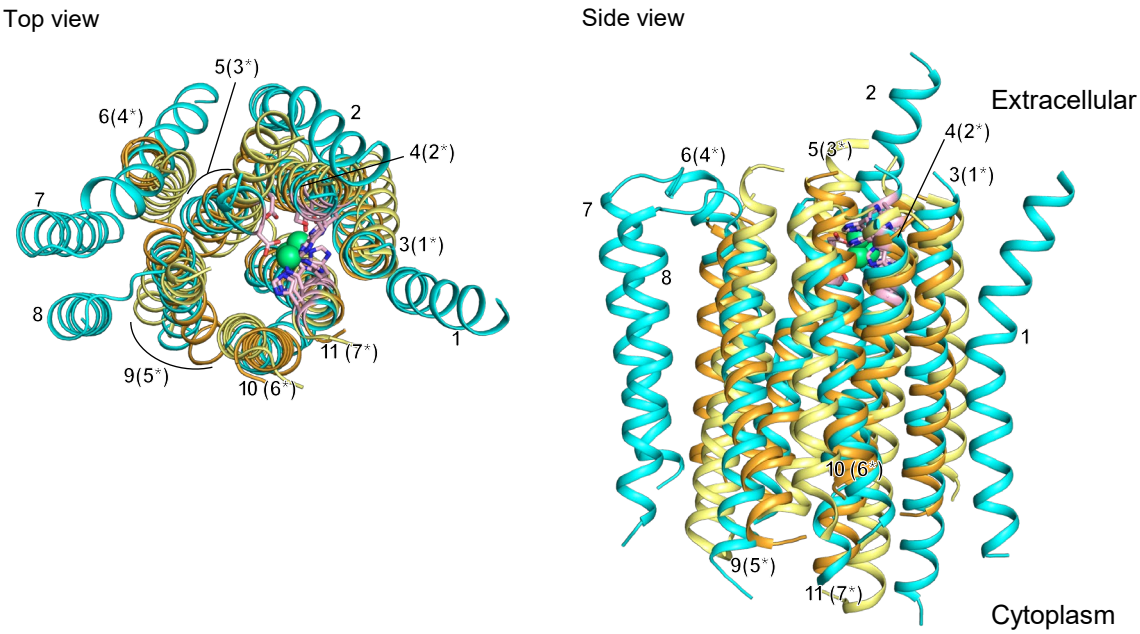

Supplementary Fig. 8 The TM domain of SIDT1 has a structural similarity with ACERs and ADIPORs.

Pairwise structure comparisons between the closed form of SIDT1 and Adiponectin receptor 2 (ADIPOR2, PDB ID: 5LX9) or Alkaline ceramidase 3 (ACER3, PDB: 6G7O) 7 TMs were performed using DALI server[20]. 7 out of 11 TMs in SIDT1 (cyan) were superimposed with all 7 TMs in AIPOR2 (yellow) and ACER3 (orange) with an overall r.m.s. d. of 3.4 Å and 4.5 Å for Cα atoms, respectively. The transmembrane segments with numbering of SIDT1 are indicated, while those of ACER3 and ADIPOR are indicated in parentheses. Extracellular domains and loops are omitted for clarification. Catalytic residues and Zn^{2+} ions are shown in pink stick model and sphere model, respectively.

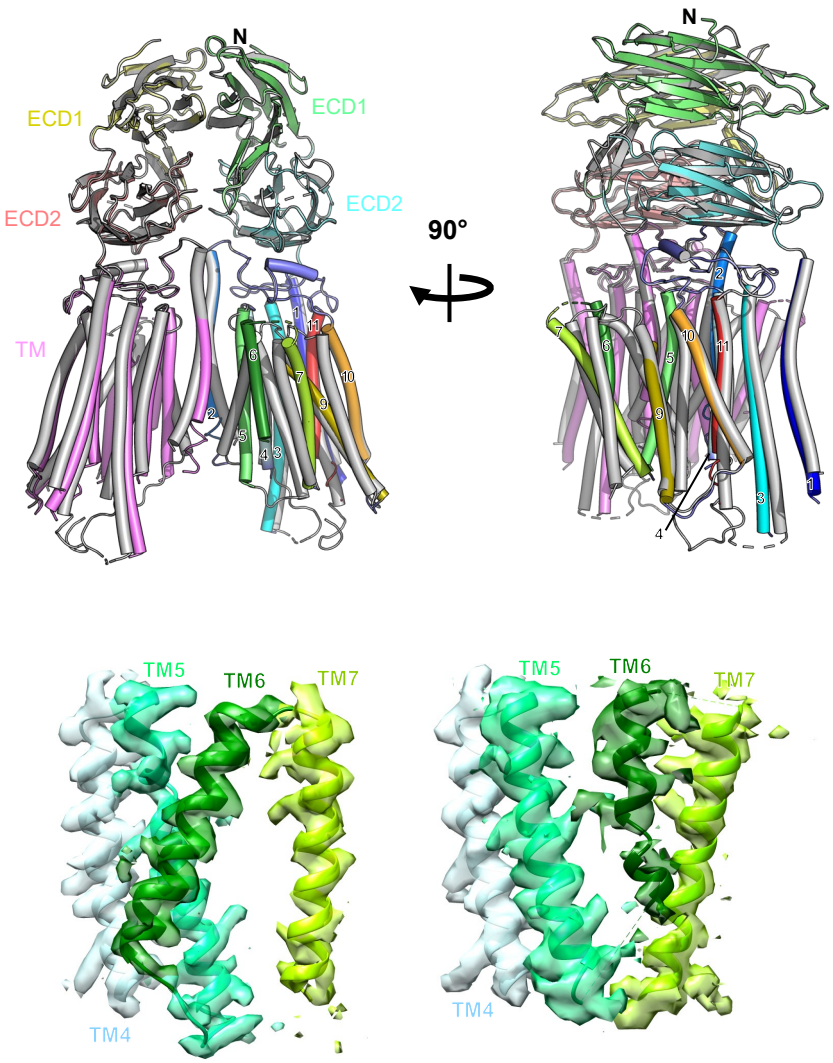

Supplementary Fig. 9 The closed-open interconversion of the SIDT1 TM region.
Pairwise structure comparisons between the closed- and open form of SIDT1. The cryo-EM density map if TM5, TM6 and TM7 which undergo significant conformation change are shown.

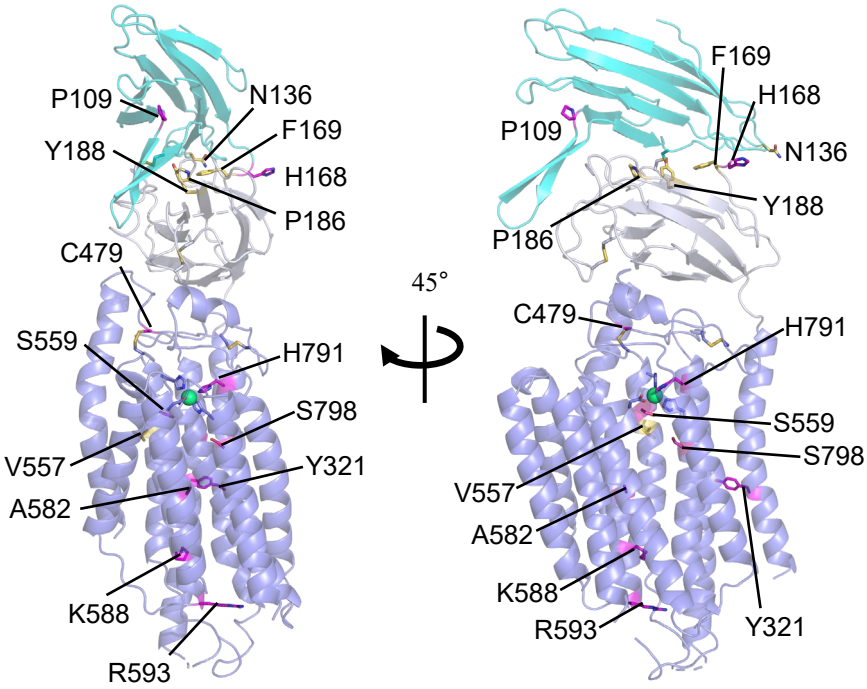

Res.	human	RNAi phenotype	position	properties
M1I	M1	weak	N-terminus	disordered
P108S	P109	strong	ECD1	buried. cis configuration
D130N	N136	weak	ECD1	exposed
R172W	H168	strong	ECD1-ECD2 linker	exposed
A173T	F169	weak	ECD1-ECD2 linker	facing to dimer interface, not involved in dimer interface
P199L	P186	weak	ECD2	facing to dimer interface, not involved in dimer interface
G201E	Y188	weak	ECD2	facing to dimer interface, not involved in dimer interface
G201R	Y188	strong	ECD2	facing to dimer interface, not involved in dimer interface
P328L	Y321	strong	TM1	hydrogen bind with main chain carboxy group of L506 (TM3)
C464Y	C479	strong	TM2-TM3	TM3 loop, disulfide bond with C565
G488E	G503	strong	TM3	buried in the protein. May disturb the protein conformation
G493R	G508	strong	TM3	buried in the protein. May disturb the protein conformation
I534N	V557	weak	TM4	exposed
S536I	S559	strong	TM4	Putative catalytic residue
C559Y	A582	strong	TM5	bulky residue may disturb the TM domain conformation
R565C	K588	strong	TM5	cation-π interaction with Phe545 (TM4)
R570C	R593	strong	TM5	Salt bridge with Glu737
H740Y	H791	strong	TM11	Zn-binding
G747R	S798	strong	TM11	near Zn-binding site

Supplementary Fig. 10 Mapping of mutations that attenuate systemic RNA by SID-1 on the structure of SIDT1.

Mutations that attenuate systemic RNA by SID-1 are mapped on the structure of SIDT1 (upper panel). Mutations of SID-1 and their properties are listed (lower panel).

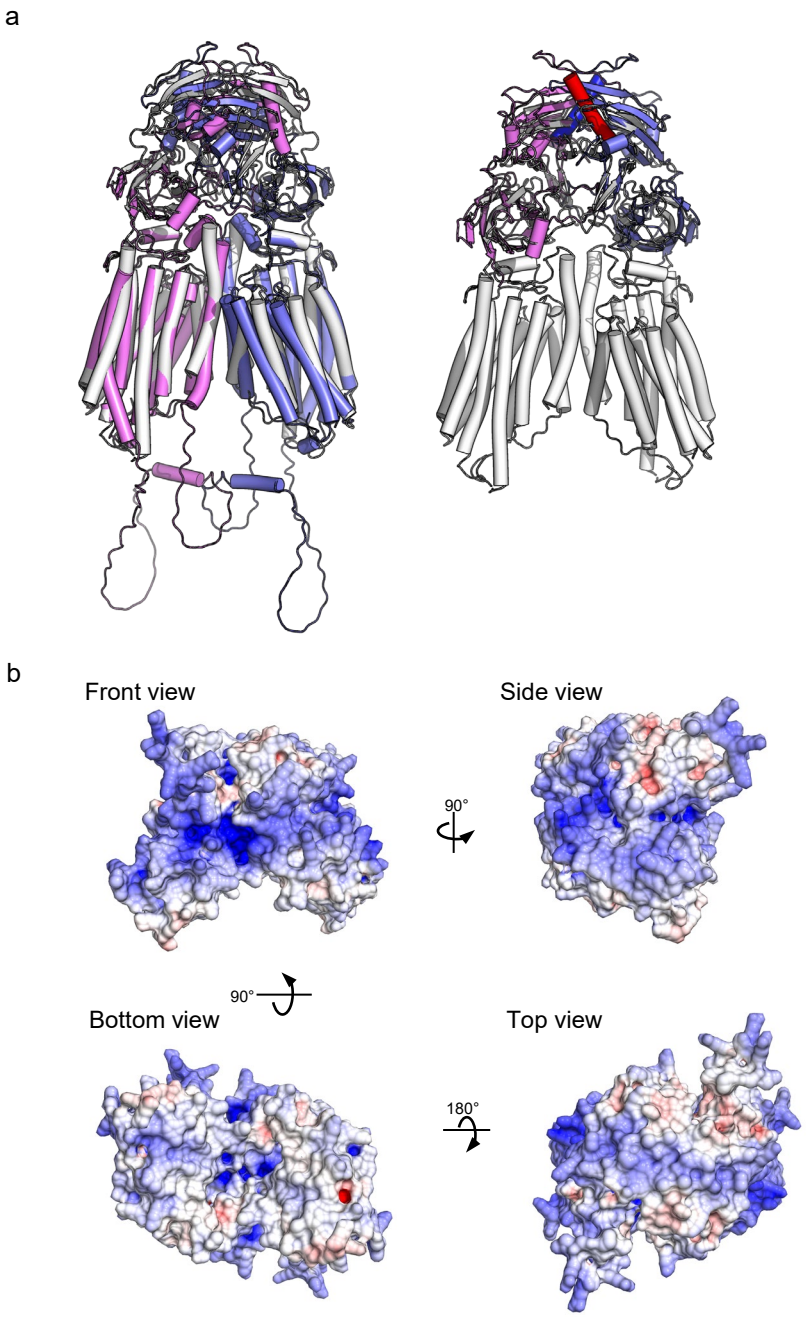

Supplementary Fig. 11 The electrostatic surface potential of predicted structure of C. elegans SID-1.

(a) Two C. elegans SID-1 structures predicted by Alpha-Fold (magenta and purple) were each superimposed on each protomer of hSIDT1 homodimer closed-form (white) (left panel). The TM region of SID-1 is relatively fit to that of SIDT1, while the extracellular domain (ECD) is not fitted well and conflicts with the other protomer due to the difference of the orientation between ECD and TM. On the other hand, when ECDs of two SID-1 structures were each superimposed on each ECD of SIDT1 homodimer (right panel), SID-1 ECDs were well fitted to SIDT1 with less confliction except for the N-terminal helix (red and blue). The N-terminal helix (residue 2-16) is connected to ECD via flexible linker (residues 17-30), which suggests that the orientation of the N-terminal helix is flexible. (b) The electrostatic surface potential of the ECD dimer model of SID-1 as right panel in (a) is shown in the same orientation as Figure 4a for comparison with SIDT1. The N-terminal 30 residues in SID-1 are omitted in the model for clarity.

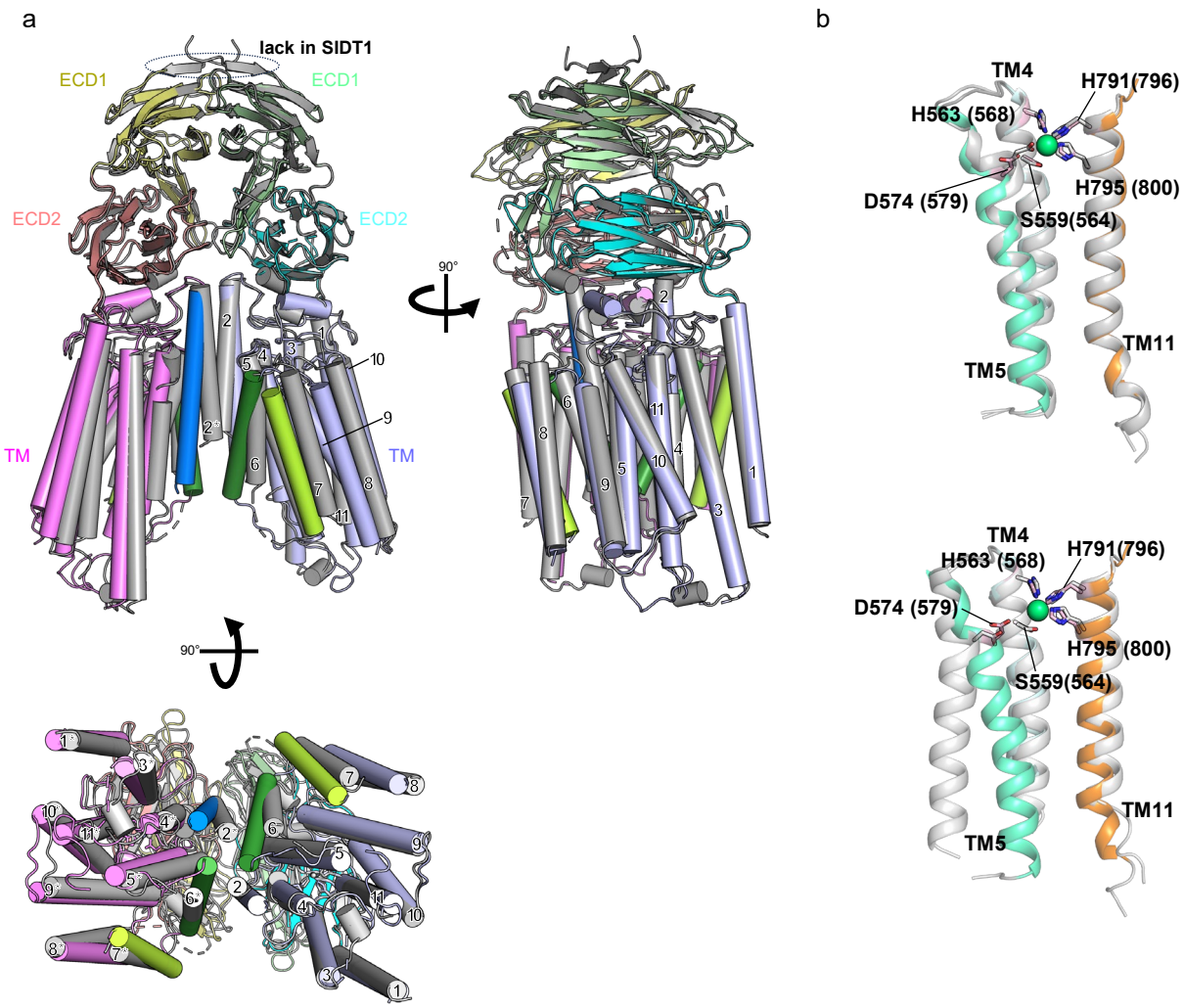

Supplementary Fig. 12 | The structural comparison between SIDT1 and SIDT2.

a. Superposition of human SIDT1 (closed-form) and human SIDT2 (gray, PDB: 7Y63) are shown. The TM numbers of the superimposed protomer are shown, but * is added to the number of the other protomer for clarity. SIDT1 lacks the first β-strand in ECD1 but has a longer TM2 and TM6 helices. Structural deviation of Cα atoms in TM6, TM7 and TM8 are higher than other regions.

b. Structural comparison focused on the catalytic site. Catalytic residues of human SIDT2 are superimposed on those of human SIDT1 closed-form (top panel) or SIDT1 open-form (bottom panel). Catalytic residues are shown with stick models and the zinc ion is shown as green sphere. Residue numbers of SIDT1 are indicated while those of SIDT2 are indicated in parentheses.